

# LEADING ORDER PQCD HADRON PRODUCTION AND NUCLEAR MODIFICATION FACTORS AT RHIC AND THE LHC \*

Ivan Vitev<sup>†</sup>

<sup>†</sup> Department of Physics and Astronomy  
Iowa State University, Ames, IA 50011  
E-mail: ivitev@iastate.edu

## Abstract

Hadron production in leading order pQCD is reviewed. The shape of the single inclusive particle spectra is well described for  $p_T \geq 2 - 3$  GeV at center of mass energies from 20 GeV to 2 TeV. The phenomenological K-factor is found to decrease systematically with  $\sqrt{s}$ . For ultra-relativistic heavy ion reactions the calculation is augmented with the effects of initial multiple parton scattering and final state radiative energy loss. Baseline CERN-LHC predictions for hadron production in  $p + p$  and suppression in central  $Pb + Pb$  reactions at  $\sqrt{s} = 5.5$  TeV are given in comparison to the corresponding results at BNL-RHIC and CERN-SPS energies.

## 1. INTRODUCTION

One of the main goals of the upcoming  $p + p$  program at  $\sqrt{s} = 14$  TeV at the Large Hadron Collider (LHC) at CERN is the unambiguous discovery of the Higgs boson, predicted by the standard model of particle interactions, as well as the search for physics that reaches beyond our current understanding of the constituents of matter and the force mediators. Equally important, however, is the continuing effort to investigate the strong sector of the SM and probe experimentally some of the fundamental predictions of QCD: the deconfinement phase transition and chiral symmetry restoration. To order  $(\alpha_s^{LO})^2$  the strong coupling constant  $\alpha_s = g_s^2/4\pi$  reads

$$\alpha_s(Q^2, n_f) = \alpha_s^{LO}(Q^2, n_f) \left[ 1 - \frac{1}{4\pi} \frac{102 - \frac{38}{3}n_f}{11 - \frac{2}{3}n_f} \alpha_s^{LO}(Q^2, n_f) \ln \ln \frac{Q^2}{\Lambda_{QCD}^2} \right], \quad (1)$$

where the lowest order  $\alpha_s^{LO}(Q^2, n_f) = 4\pi / \left( 11 - \frac{2}{3}n_f \right) \ln \frac{Q^2}{\Lambda_{QCD}^2}$ . QCD is thus “asymptotically free”, i.e. for  $n_f \leq 6$  the running coupling, Eq. (1), approaches zero in the limit of large momentum transfer  $Q$ , - a general feature of non-Abelian gauge theories with sufficiently small number of fermions. In hot and dense matter the typical momentum scale is on the order of the temperature  $Q \sim T$ , assuming local thermal equilibrium. Large initial temperatures and energy densities can be experimentally achieved in ultra-relativistic heavy ion reactions. The  $Pb + Pb$  program at  $\sqrt{s_{NN}} = 5.5$  TeV at the LHC is targeted at the search for the quark-gluon plasma (QGP) [1] and the study of its properties. The Bjorken-estimated  $T_i \simeq 1$  GeV for these conditions exceeds by a large margin the current lattice QCD results for the critical temperature  $T_c \simeq 170$  MeV. An important advantage of the LHC is that it will ultimately make small- $x$  physics studies in heavy ion collisions feasible (not applicable at RHIC except possibly for  $p_T < 0.5$  GeV). At very small values of  $x$  the rapid growth of the gluon distribution in nucleons and

---

\* Contribution to the CERN Yellow Report on Hard Probes in Heavy Ion Collisions at the LHC. This manuscript also provides details on the background calculations for Ref. [4] and discussion on results that have been omitted there due to space limitations.

nuclei is tamed by absorption terms that lead to a modification [2] of the DGLAP evolution equations and correct the small- $x$  unitarity problem:

$$\begin{aligned} \frac{\partial x G(x, Q^2)}{\partial \ln Q^2} &= \frac{C_A \alpha_s}{\pi} \int_x^1 \frac{dx'}{x'} \frac{x}{x'} \gamma^{gg} \left( \frac{x}{x'} \right) x' G(x', Q^2) \\ &\quad - \frac{4\pi^3}{N_c^2 - 1} \left( \frac{C_A \alpha_s}{\pi} \right)^2 \frac{1}{Q^2} \int_x^1 \frac{dx'}{x'} (x')^2 G^{(2)}(x', Q^2), \end{aligned} \quad (2)$$

where  $\gamma^{gg}$  is the gluon splitting function and  $G^{(2)}(x, Q^2)$  is proportional to the gluon density overlap. An opportunity to test these predictions at the LHC is provided by the  $p + Pb$  program at  $\sqrt{s} = 8.8$  TeV since it stands the best chance of identifying initial state nuclear effects [3] and separating them [4] from the final state multi-parton interactions.

The search of novel physical effects in ultra-relativistic heavy ion reactions at the LHC can only rely on a detailed comparison between the experimental data and the projected current, or “conventional”, knowledge. This calls for detailed baseline calculations of jet and hadron production at those center of mass energies as well as an estimate of the known nuclear effects. The purpose of this manuscript is to present a *lowest order* (LO) analysis of inclusive hadron production up to the Tevatron energies and discuss hadron differential cross sections and composition at the LHC. This choice is dictated by the requirement of self-consistent incorporation of nuclear effects that are at present computed/parameterized to LO. It also complements next-to-leading order (NLO) calculations of jet and hadron production [5, 6]. Evaluation of the nuclear modification factors at the LHC in comparison to RHIC and discussion of the hadron composition is also presented. Results on Cronin and shadowing effects are given at forward (in the direction of the proton/deuteron beam)  $y = +3$  rapidity.

## 2. HADRON PRODUCTION IN FACTORIZED PQCD

The standard factorized pQCD hadron production formalism expresses the differential hadron cross section in  $N + N \rightarrow h + X$  as a convolution of the measured parton distribution functions (PDFs)  $f_{\alpha/N}(x_\alpha, Q_\alpha^2)$  for the interacting partons ( $\alpha = a, b$ ), with the fragmentation function (FFs)  $D_{h/c}(z, Q_c^2)$  for the leading scattered parton  $c$  into a hadron of flavor  $h$  and the parton-parton differential cross sections for the elementary sub-process  $d\sigma^{(ab \rightarrow cd)}/d\hat{t}$ :

$$\begin{aligned} E_h \frac{d\sigma^{NN}}{d^3p} &= K_{NLO} \sum_{abcd} \int_0^1 dz_c \int_{x_{a \min}}^1 \int_{x_{b \min}}^1 dx_a dx_b f_{a/p}(x_a, Q_a^2) f_{b/p}(x_b, Q_b^2) \\ &\quad \times D_{h/c}(z_c, Q_c^2) \frac{\hat{s}}{\pi z_c^2} \frac{d\sigma^{(ab \rightarrow cd)}}{d\hat{t}} \delta(\hat{s} + \hat{u} + \hat{t}). \end{aligned} \quad (3)$$

A list of the lowest order partonic cross sections can be found in [7]. In Eq. (3)  $x_a, x_b$  are the initial momentum fractions carried by the interacting partons and  $z_c = p_h/p_c$  is the momentum fraction of the observed hadron.  $K_{NLO}$  is a phenomenological factor that is meant to account for next-to-leading order (NLO) corrections. It is  $\sqrt{s}$  and scale dependent and takes typical values  $\simeq 1 - 4$ . One usually finds that Eq. (3) over-predicts the curvature of the inclusive hadron spectra  $|\partial_{p_T} d\sigma^h|$  at transverse momenta  $p_T \leq 4$  GeV. This can be partly corrected by the introduction of a small intrinsic (or primordial)  $k_T$ -smearing of partons, transversely to the collision axis, and generalized parton distributions  $\tilde{f}_\alpha(x, k_T, Q^2)$  motivated by the pQCD initial state radiation. For the corresponding modification of the kinematics in (3) in addition to the  $\int d^2k_T^a \int d^2k_T^b (\dots)$  integrations see [7]. The generalized parton distributions are often approximated as

$$\tilde{f}_\alpha(x, k_T, Q^2) \approx f_\alpha(x, Q^2) g(k_T), \quad g(k_T) = \frac{e^{-k_T^2/\langle k_T^2 \rangle}}{\pi \langle k_T^2 \rangle}, \quad (4)$$

where the width  $\langle k_T^2 \rangle$  of the Gaussian enters as a phenomenological parameter.

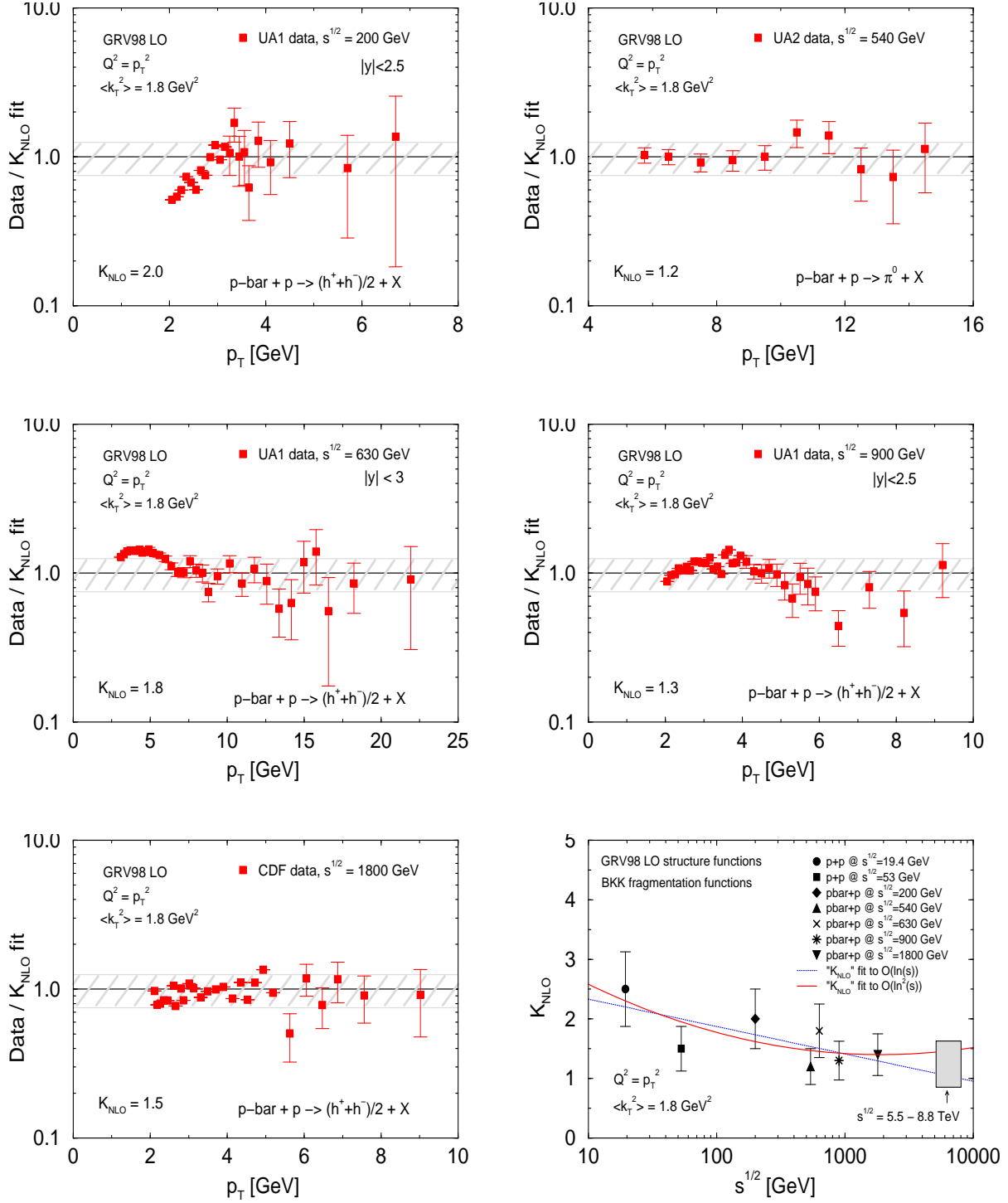


Fig. 1: Extracted  $K_{\text{NLO}}$  from comparison of LO pQCD calculation to data [10, 11, 12, 13, 14, 15] at and about mid-rapidity in the range  $2 \leq p_T \leq 25$  GeV. A systematic decrease of  $K_{\text{NLO}}$  with  $\sqrt{s}$  is observed and illustrated in the bottom right panel. The projected 50% uncertainty at  $\sqrt{s} = 5.5 - 8.8$  TeV is also shown.

Perturbative QCD fits to data [8, 9, 10, 11, 12, 13, 14, 15] use different coupled choices for  $K_{NLO}$  and  $\langle k_T^2 \rangle$  and the extracted values are thus not directly comparable. However, similar agreement between data and theory at the level of spectral shapes and the  $\sqrt{s}$  dependence of the corrective factors discussed above is found. In [16] the factorization and fragmentation scales were set to  $Q_{PDF} = p_T/2$  and  $Q_{FF} = p_T/2z_c$  and no  $K_{NLO}$  factors were employed. The extracted  $\langle k_T^2 \rangle$  decreases from  $2.7 \text{ GeV}^2$  at  $\sqrt{s} \simeq 50 \text{ GeV}$  to  $0.75 \text{ GeV}^2$  at  $\sqrt{s} \simeq 2 \text{ TeV}$ . Alternatively, in [17] no primordial  $k_T$ -smearing was used and the scales in the calculation were fixed to be  $Q_{PDF} = Q_{FF} = p_T$ . The deduced  $K_{NLO}$  decreases from  $\sim 6$  at  $\sqrt{s} \simeq 50 \text{ GeV}$  to  $\sim 1.5$  at  $\sqrt{s} \simeq 2 \text{ TeV}$ .

In the fits shown in Fig. 1 we have used the GRV98 LO PDFs [18] and the BKK LO FFs [19]. Proton+antiproton fragmentation has been parameterized as in [20], inspired from PYTHIA [21] results. A fixed  $\langle k_T^2 \rangle_{pp} = 1.8 \text{ GeV}^2$  has been employed, leading to a  $K_{NLO}$  parameter that naturally exhibits a smaller variation with  $\sqrt{s}$ . A  $\pm 25\%$  error band about the  $K_{NLO}$  value, fixed by the requirement to match the moderate- and high- $p_T$  behavior of the data, is also shown. The fragmentation and factorization scales were fixed as in [17]. In the lower right panel the systematic decrease of the next-to-leading order K-factor is presented. Two fits to  $K_{NLO}$  have been used: linear  $K_{NLO} = 2.7924 - 0.0999 \ln s$  and quadratic  $K_{NLO} = 3.8444 - 0.3234 \ln s + 0.0107 \ln^2 s$  in  $\ln s$ . For center of mass energies up to 1 TeV the two parameterization differ by less than 15% but this difference is seen to grow to 30%-50% at  $\sqrt{s} = 5 - 10 \text{ TeV}$ .

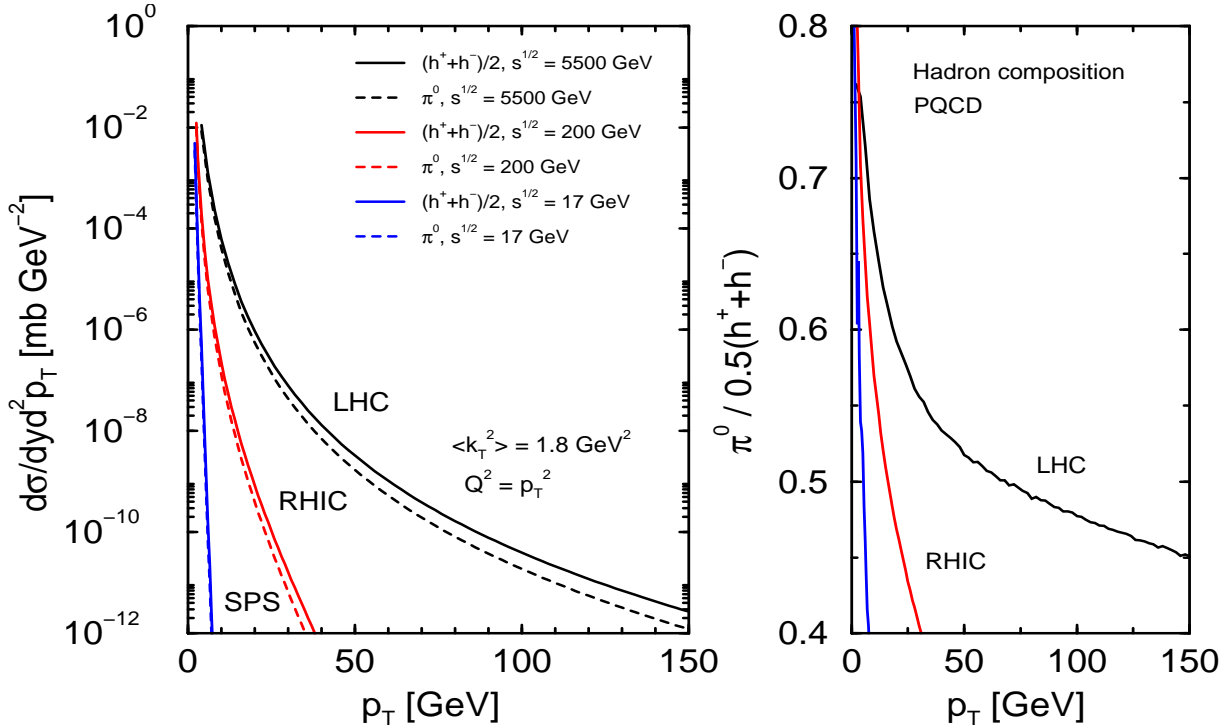


Fig. 2: The predicted LO differential cross section  $d\sigma^{pp}/dy d^2p_T$  for inclusive neutral pion and charged hadron production at midrapidity  $y = 0$  in  $p + p$  ( $\bar{p} + p$ ) reactions is shown for  $\sqrt{s} = 17, 200$ , and  $5500 \text{ GeV}$ . The ratio of neutral pions to inclusive charged hadrons versus  $p_T$  is given in the right panel.

In Fig. 2 the predicted transverse momentum distribution of neutral pions and inclusive charged hadrons is shown, corresponding to the quadratic in  $\ln s$  fit to  $K_{NLO}$  for energies typical of SPS, RHIC, and the LHC. The *significant* hardening of the spectra with  $\sqrt{s}$  has two important consequences for  $p + A$

and  $A + A$  collisions: a notably reduced sensitivity to initial state kinematic effects (smaller Cronin) and larger variation of the manifested final-state multi-parton scattering (energy loss) with  $p_T$  [4]. We have also investigated the effect of isospin asymmetry between  $p + p$  and  $p + \bar{p}$  reactions in  $\pi^0$  and  $h^+ + h^-$  production and found it to be small. More quantitatively, at  $\sqrt{s} = 5.5$  TeV the fractional difference  $|d\sigma^{\bar{p}p} - d\sigma^{pp}|/d\sigma^{pp}$  varies from 2.5% at  $p_T = 5$  GeV to 4.8% at  $p_T = 150$  GeV. This is insignificant as compared to the projected 50% uncertainty that comes from the extrapolation of  $K_{NLO}$  in LO calculations (see Fig. 1) or the choice of scale in NLO calculations. A recent study showed *no* deviation from DGLAP evolution, Eq. (2), at  $Q^2 = 10$  GeV<sup>2</sup> down to  $x = 10^{-5}$  in  $N + N$  reactions [22]. The nuclear amplification effect  $\propto A^{1/3} \simeq 10$  for a large nucleus is still insufficient to enable measurements of high initial gluon density QCD at RHIC, but will play an important role at the LHC.

## 2.1 Perturbative QCD hadron composition

The predicted hadron composition in  $p + p$  ( $\bar{p} + p$ ) reactions is plotted in the right panel of Fig. 2. The proton+kaon fraction is seen to increase systematically with  $p_T$  ( $x_T = 2p_T/\sqrt{s}$ ) and is reflected in the decreasing  $\pi^0/0.5(h^+ + h^-)$ . At RHIC and LHC energies this ratio becomes  $\sim 0.5$  at  $p_T \simeq 15$  GeV and  $p_T \simeq 75$  GeV, respectively. At transverse momenta  $p_T \simeq 2 - 4$  GeV the contribution of baryons and kaons to  $h^+ + h^-$  is  $\leq 20\%$ . This is significantly smaller compared to data on  $N + N$  reactions, with the discrepancy being amplified in central  $A + A$ . Possible explanations include: enhanced baryon production via topological gluon configurations (junctions) and its interplay with jet quenching [23, 24] in  $A + A$  [25, 26], hydrodynamic transverse flow [27], uncertainty of the fragmentation functions  $D_{p/c}(z_c, Q^2)$  into protons and antiprotons [28], and quark recombination driven by unorthodox (extracted) parton distributions inside nuclei [29]. The approaches in Refs. [25, 26, 27] also address the centrality dependence of the baryon/meson ratios in heavy ion collisions at RHIC. In [26] it has been shown that similar nuclear enhancement is expected in  $\Lambda, \bar{\Lambda}$  production (as compared to kaons). The combined low- $p_T$  baryon enhancement and the growth of the non-pionic hadron fraction in the perturbative regime may lead to an approximately constant pion to charged hadron ratio in the full measured  $p_T$  region at RHIC at  $\sqrt{s}_{NN} = 200$  GeV. We propose that the LHC may play a critical role in resolving the mystery of enhanced baryon production in  $A + A$  through the significantly larger experimentally accessible  $p_T$  range. Effects associated with baryon transport and transverse flow are not expected to extend beyond  $p_T = 10 - 15$  GeV and may result in a detectable minimum of the baryon/meson ratio versus  $p_T$  before a secondary subsequent rise. On the other hand, fragmentation functions (possibly enhanced at large  $z_c$  relative to current parameterizations) are expected to exhibit a much more monotonic behavior.

## 3. NUCLEAR MODIFICATION FACTORS

Dynamical nuclear effects in  $p + A$  and  $A + A$  reactions are detectable through the nuclear modification ratio

$$R_{BA}(p_T) = \begin{cases} \frac{d\sigma^{pA}}{dyd^2p_T} / \frac{A d\sigma^{pp}}{dyd^2p_T} & \text{in } p + A \\ \frac{dN^{AA}(b)}{dyd^2p_T} / \frac{T_{AA}(b) d\sigma^{pp}}{dyd^2p_T} & \text{in } A + A \end{cases}, \quad (5)$$

where  $A$  and  $T_{AA}(b) = \int d^2\mathbf{r} T_A(\mathbf{r})T_B(\mathbf{r} - \mathbf{b})$  in terms of nuclear thickness functions  $T_A(r) = \int dz \rho_A(\mathbf{r}, z)$  are the corresponding Glauber scaling factors [30] of  $d\sigma^{pp}$ . We note that in  $R_{BA}(p_T)$  the uncertainty associated with the  $K_{NLO}$  factors, discussed in the previous section, drops out. The reference calculations that follow include shadowing/antishadowing/EMC-effect (here referred to as “shadowing”), the Cronin effect, and the non-Abelian energy loss of jets. The scale dependent nuclear PDFs read:  $f_{\alpha/A}(x, Q^2) = S_{\alpha/A}(x, Q^2) (Z/A f_{\alpha/p}(x, Q^2) + N/A f_{\alpha/n}(x, Q^2))$ , where we take the isospin effects on average and the EKS’98 parameterization [31] of the shadowing functions  $S_{\alpha/A}(x, Q^2)$ . Initial state multiple elastic scatterings have been discussed in [32, 33, 34]. From [34] the transverse momentum

distribution of partons that have undergone an average  $\chi = L/\lambda$  incoherent interactions in the medium can be evaluated exactly for any initial flux  $dN^{(0)}(\mathbf{p})$ :

$$dN(\mathbf{p}) = \sum_{n=0}^{\infty} e^{-\chi} \frac{\chi^n}{n!} \int \prod_{i=1}^n d^2 \mathbf{q}_i \frac{1}{\sigma_{el}} \frac{d\sigma_{el}}{d^2 \mathbf{q}_i} dN^{(0)}(\mathbf{p} - \mathbf{q}_1 - \dots - \mathbf{q}_n). \quad (6)$$

Numerical estimates of (6) show that for thin media with a few semi-hard scatterings the induced transverse momentum broadening exhibits a weak logarithmic enhancement with  $p_T$  and is proportional to  $L \propto A^{1/3}$ . The transverse momentum transfer per unit length in cold nuclear matter is found to be  $\mu^2/\lambda \simeq 0.05 \text{ GeV}^2/\text{fm}$  [4] from comparison to low energy  $p + A$  data [8, 9, 10]. The left top and bottom panels of Fig. 3 show the predicted Cronin+shadowing effect in  $p + Pb$  collisions at  $\sqrt{s} = 8.8 \text{ TeV}$  and central  $Pb + Pb$  at  $\sqrt{s} = 5.5 \text{ TeV}$  without final state medium induced energy loss. The 4% (10%) enhancement of  $R_{BA}$  at  $p_T \simeq 40 \text{ GeV}$  comes from antishadowing and is not related to multiple initial state scattering. The observed difference between  $\pi^0$  and  $0.5(h^+ + h^-)$  reflects the different  $S_\alpha(x, Q^2)$  for quarks and gluons. Cronin effect at the LHC results in slowing down of the decrease of  $R_{BA}$  at small  $x$  as seen in the  $p_T \rightarrow 0$  limit. In contrast, at RHIC one finds  $\simeq 30\%$  enhancement in  $d + Au$  reactions at  $\sqrt{s} = 200 \text{ GeV}$  and  $\simeq 60\%$  effect in central  $Au + Au$  relative to the *binary collision* scaled  $p + p$  result. At CERN-SPS energies of  $\sqrt{s} = 17 \text{ GeV}$  the results are most striking, with values reaching 250% in  $d + Au$  and 400% in central  $Au + Au$  at  $p_T \simeq 4 \text{ GeV}$ . For a summary of results on midrapidity Cronin effect at the LHC see [35].

The manifestation of multiple initial state scattering and nuclear shadowing at forward and backward rapidities  $y = \pm 3$  in  $p + Pb$  at the LHC (for CMS  $\eta \leq 2.5$ ) and  $d + Au$  at RHIC (for BRAHMS  $\eta \leq 3$ ) has also been studied in the framework of a fixed (or slowly varying) initial parton interaction strength. At LHC energies at  $y = +3$  (in the direction of the proton beam) the effect of the sequential projectile interactions is again small (due to the much flatter rapidity and transverse momentum distributions) and is overwhelmed by shadowing, which is found to be a factor of 2-3 times larger than the  $y = 0$  result at small  $p_T \sim \text{few GeV}$  and vanishes ( $R_{BA} = 1$ ) at  $p_T \simeq 50 \text{ GeV}$ . As previously emphasized, initial state gluon showering can significantly change the low- $p_T$  behavior of the hadronic spectra at the LHC beyond the current shadowing parameterization. At RHIC in  $d + Au$  reactions at  $\sqrt{s} = 200 \text{ GeV}$  the nuclear modification ratio is qualitatively different. While near nucleus beam (backward  $y = -3$ ) rapidity  $R_{BA} \simeq 0.9 - 1$  at forward rapidities  $y = +3$  the nuclear modification factor exhibits a much more dramatic  $p_T$  dependence. At small transverse momenta  $p_T \sim 1 \text{ GeV}$  hadron production is suppressed relative to the binary collision scaled  $p + p$  result,  $R_{BA} \leq 0.8$ . The maximum Cronin enhancement  $R_{BA}^{\text{max}} \simeq 1.3$  (30%) is essentially the same as at midrapidity [4] but slightly shifted to larger  $p_T$ . We emphasize that *both* the suppression and enhancement regions are an integral part of the Cronin effect [8, 9, 10] that is understood in terms of probability conservation and momentum redistribution resulting from multiple initial state scattering [4, 16, 30, 32, 33, 34, 35]. At forward (in the direction of the deuteron beam) rapidities a calculation as in [4] demonstrates a *broad* Cronin enhancement region with  $R_{BA} \simeq 25\%$  at  $p_T = 5 \text{ GeV}$ . This is understood in terms of the significantly steeper fall-off of the hadron spectra away from midrapidity that enhances the effect of the otherwise similar transverse momentum kicks. While the discussed moderate  $p_T$  interval lies at the very edge of BRAHMS acceptance (at  $y = +3$ ) the same qualitative picture holds at  $y = +2$ .

The full solution for the medium induced gluon radiation off jets produced in a hard collisions inside the nuclear medium of length  $L$  and computed *to all orders* in the correlations between the multiple scattering centers via the GLV reaction operator approach [36] can be written as ( $x = k^+/p^+ \approx \omega/E$ )

$$\sum_{n=1}^{\infty} x \frac{dN^{(n)}}{dx d^2 \mathbf{k}} = \frac{C_{R\alpha_s}}{\pi^2} \sum_{n=1}^{\infty} \prod_{i=1}^n \int_0^{L - \sum_{a=1}^{i-1} \Delta z_a} \frac{d\Delta z_i}{\lambda_g(i)} \int \prod_{i=1}^n \left( d^2 \mathbf{q}_i \left[ |\bar{v}_i(\mathbf{q}_i)|^2 - \delta^2(\mathbf{q}_i) \right] \right)$$

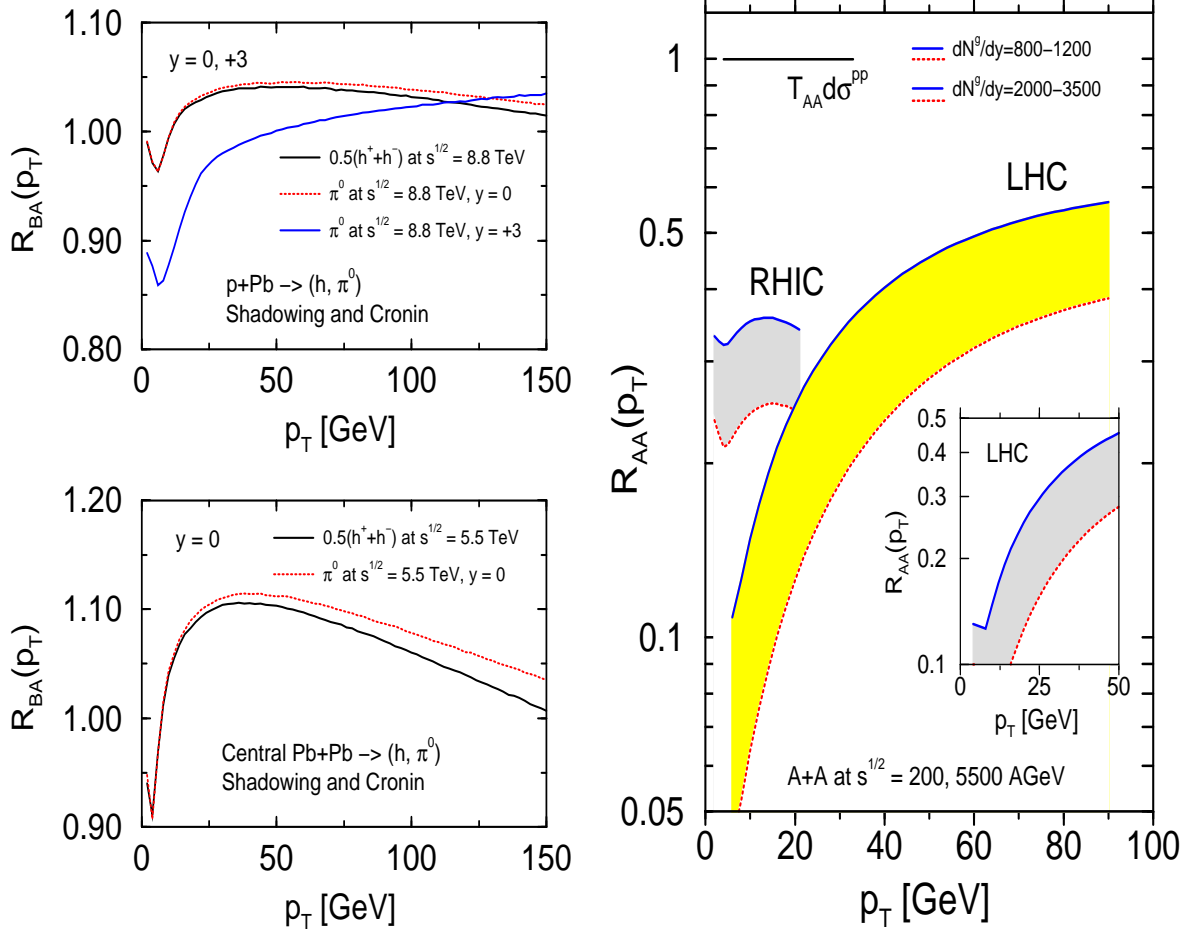


Fig. 3: The antishadowing and Cronin effects in  $p + Pb$  and central  $Pb + Pb$  without energy loss at the LHC ( $\sqrt{s} = 5.5$  and 8.8 TeV) are shown in the left top and bottom panels. The right panel demonstrates the dominance of final state radiative energy loss effects at the LHC with a much stronger  $p_T$  dependence compared to RHIC. The possible restoration of the participant scaling through hydrodynamic-like feedback at  $p_T \rightarrow 0$  is also shown [4].

$$\begin{aligned}
& \times \left( -2 \mathbf{C}_{(1,\dots,n)} \cdot \sum_{m=1}^n \mathbf{B}_{(m+1,\dots,n)(m,\dots,n)} \right. \\
& \times \left[ \cos \left( \sum_{k=2}^m \omega_{(k,\dots,n)} \Delta z_k \right) - \cos \left( \sum_{k=1}^m \omega_{(k,\dots,n)} \Delta z_k \right) \right] \Bigg) , \quad (7)
\end{aligned}$$

where  $\sum_2^1 \equiv 0$  is understood. In (7)  $\mathbf{C}_{(m,\dots,n)} = \frac{1}{2} \nabla_{\mathbf{k}} \ln(\mathbf{k} - \mathbf{q}_m - \dots - \mathbf{q}_n)^2$ ,  $\mathbf{B}_{(m+1,\dots,n)(m,\dots,n)} = \mathbf{C}_{(m+1,\dots,n)} - \mathbf{C}_{(m,\dots,n)}$  are the color current propagators,  $\omega_{(m,\dots,n)}^{-1} = 2xE/|C_{(m,\dots,n)}^2|$  are formation times, and  $\Delta z_k = z_k - z_{k-1}$  are the separations of subsequent scattering centers. The momentum transfers  $\mathbf{q}_i$  are distributed according to a normalized elastic scattering cross section  $|\bar{v}_i(\mathbf{q}_i)|^2 = \sigma_{el}^{-1} d\sigma_{el}/d^2\mathbf{q}_i$  and the radiative spectrum can be evaluated from (7) for any initial nuclear geometry with an arbitrary subsequent dynamical evolution of the matter density. At large jet energies the lowest order correlation between the jet production point one of the scatterings that follow has been shown to dominate and lead to a quadratic mean energy loss dependence on the size of the plasma,  $\Delta E \propto L^2$  for *static* media [37]. To improve the numerical accuracy for small parton energies we include corrections to third order in opacity [4]. The dynamical expansion of the bulk soft matter is assumed to be of Bjorken type. For a summary of results from recent non-Abelian energy loss calculations see [38].

In the Poisson approximation of independent gluon emission [39, 40, 41, 42] the probability distribution  $P(\epsilon, E)$  of the fractional energy loss  $\epsilon = \sum_i \omega_i/E$  can be obtained iteratively from the single inclusive gluon radiation spectrum  $dN(x, E)/dx$  [40]. If a fast parton loses  $\epsilon E$  of its initial energy prior to hadronization its momentum fraction  $z_c$  is modified to  $z_c^* = p_h/p_c(1 - \epsilon) = z_c/(1 - \epsilon)$ . The observable suppressed hadron differential cross section can be computed from Eq. (3) with the substitution

$$D_{h/c}(z_c, Q^2) \longrightarrow \int d\epsilon P(\epsilon, p_c) \frac{z_c^*}{z_c} D_{h/c}(z_c^*, Q^2). \quad (8)$$

The nuclear modification factor  $R_{AA}(p_T)$  at the LHC is shown on the right panel of Fig. 3 and is completely dominated by final state interactions (see left panel). It shows a *significantly stronger*  $p_T$  dependence as compared to RHIC, where jet quenching was predicted to be *approximately constant* over the full measured moderate- to high-transverse momentum range [4], the result of an interplay of shadowing, Cronin effect, and radiative energy loss. The variation of  $R_{AA}$  at the LHC is a factor of 5: from 10-20 fold suppression at  $p_T = 10$  GeV to only a factor 2-3 suppression at  $p_T = 100$  GeV. The reason for such a prominent variation is the hardening of the particle transverse momentum spectra and the insufficient balancing action of multiple initial state scatterings. In fact the prediction from Fig. 3 is that the suppression in central  $Pb + Pb$  at  $\sqrt{s_{NN}} = 5.5$  TeV at  $p_T \simeq 40$  GeV is comparable to the factor of 4-5 suppression currently observed at RHIC.

The extrapolation of the LHC quenching calculations to small  $p_T \rightarrow 0$  results into suppression below participant scaling. More careful examination of the mean energy loss of partons, in particular for gluons radiating in nuclear matter at LHC densities, reveals sizable regions of phase space with  $\Delta E \geq E$ . This indicates complete absorption of jets in nuclear matter. There is experimental evidence that this regime of extreme *final state* densities may have been achieved at RHIC [43, 44, 45]. In this case Eq. (8) has to be corrected to include the feedback of the radiated gluons into the system. This hydrodynamic-like feedback is expected to recover the  $N_{part}$  scaling in the soft  $p_T$  region [4] - also illustrated on the right panel of Fig. 3. The effective initial gluon density derived from the rapidity densities used in Fig. 3 are  $\rho_g(RHIC) = 30 - 50/\text{fm}^3$  and  $\rho_g(LHC) = 130 - 275/\text{fm}^3$ . These are one to two orders of magnitude larger than the density of cold nuclear matter and are suggestive of a deconfined QCD state - the quark-gluon plasma. Interestingly, a recent study of non-equilibrium parton transport in central  $Au + Au$  and  $Pb + Pb$  at  $\sqrt{s_{NN}} = 200$  GeV and  $\sqrt{s} = 5.5$  TeV has found initial parton densities corresponding to the lower bound of the intervals quoted above.

#### 4. CONCLUSIONS

In summary, a lowest order pQCD analysis of single inclusive hadron production has been performed, revealing a systematic decrease with  $\sqrt{s}$  of the contribution of the next-to-leading corrections to the differential cross sections. The predicted  $d\sigma^h/dy d^2p_T$  exhibits significant hardening with transverse momentum and an increased fractional contribution of kaons and protons at high  $p_T$ , the latter also being true at RHIC energies. In central  $A + A$  reactions the nuclear modification factor  $R_{AA}(p_T)$  at the LHC is shown to be completely dominated by final state multi-parton interactions [4]. For comparison, at RHIC Cronin effect and nuclear shadowing also play an important role, leading to an approximately constant suppression ratio. At the SPS initial state multiple elastic scatterings dominate, resulting in a net enhancement of hadron production. At forward ( $y = +3$ ) rapidities in  $d + Au$  at RHIC the Cronin enhancement region is predicted to be broader in comparison to the  $y = 0$  case. In contrast in  $p + Pb$  at the LHC nuclear shadowing dominates but in order to detect a sizable reduction relative to the binary collision scaled  $p + p$  cross section measurements at close to proton rapidity ( $y_{\max} = 9.2$  for  $\sqrt{s} = 8.8$  TeV) are needed.

The predicted decreasing  $R_{AA}$  with  $p_T$  at the LHC, if confirmed, may have important experimental consequences. Comparative large- $E_T$  measurements of the difference in the *full structure* of the jet cone in  $p + p$  and  $A + A$  reactions may prove difficult for weak signals and large backgrounds. We emphasize



that one of the easiest and most unambiguous approaches for detecting the non-Abelian jet energy loss and performing jet-tomographic analysis of the properties of the hot and dense matter created in ultra-relativistic heavy ion reactions is through the suppression pattern of leading hadrons. Therefore these measurements should enter as an important part of the experimental programs at the LHC.

## Acknowledgments

Many helpful discussions with M. Gyulassy, K. Eskola, V. Kolhinen, J. W. Qiu, and J. Vary are gratefully acknowledged. This work is supported by the United States Department of Energy under Grant No. DE-FG02-87ER40371.

## References

- [1] J. C. Collins and M. J. Perry, Phys. Rev. Lett. **34** (1975) 1353.
- [2] A. H. Mueller and J. w. Qiu, Nucl. Phys. B **268** (1986) 427.
- [3] A. Dumitru and J. Jalilian-Marian, Phys. Rev. Lett. **89** (2002) 022301 [arXiv:hep-ph/0204028].
- [4] I. Vitev and M. Gyulassy, Phys. Rev. Lett. **89** (2002) 252301 [arXiv:hep-ph/0209161].
- [5] A. Accardi, N. Armesto and I. P. Lokhtin, *these proceedings*, arXiv:hep-ph/0211314.
- [6] I. Sarcevic, *these proceedings*; P. Levai and G.G. Barnafoldi, *these proceedings*.
- [7] J. F. Owens, Rev. Mod. Phys. **59** (1987) 465.
- [8] J. W. Cronin, H. J. Frisch, M. J. Shochet, J. P. Boymond, R. Mermoud, P. A. Piroue and R. L. Sumner, in *C74-07-01.17* Phys. Rev. D **11** (1975) 3105.
- [9] P. B. Straub *et al.*, Phys. Rev. Lett. **68** (1992) 452.
- [10] D. Antreasyan, J. W. Cronin, H. J. Frisch, M. J. Shochet, L. Kluberg, P. A. Piroue and R. L. Sumner, Phys. Rev. D **19** (1979) 764.
- [11] B. Alper *et al.* [British-Scandinavian ISR Collaboration], Phys. Lett. B **44** (1973) 521.
- [12] C. Albajar *et al.* [UA1 Collaboration], Nucl. Phys. B **335** (1990) 261.
- [13] M. Banner *et al.* [UA2 Collaboration], Z. Phys. C **27** (1985) 329.
- [14] G. Bocquet *et al.*, Phys. Lett. B **366** (1996) 434.
- [15] F. Abe *et al.* [CDF Collaboration], Phys. Rev. Lett. **61** (1988) 1819.
- [16] Y. Zhang, G. Fai, G. Papp, G. G. Barnafoldi and P. Levai, Phys. Rev. C **65** (2002) 034903 [arXiv:hep-ph/0109233].
- [17] K. J. Eskola and H. Honkanen, Nucl. Phys. A **713** (2003) 167 [arXiv:hep-ph/0205048].
- [18] M. Gluck, E. Reya and A. Vogt, Eur. Phys. J. C **5** (1998) 461 [arXiv:hep-ph/9806404].
- [19] J. Binnewies, B. A. Kniehl and G. Kramer, Z. Phys. C **65** (1995) 471 [arXiv:hep-ph/9407347].
- [20] X. N. Wang, Phys. Rev. C **58** (1998) 2321 [arXiv:hep-ph/9804357].
- [21] T. Sjostrand, Comput. Phys. Commun. **82** (1994) 74.
- [22] K. J. Eskola, H. Honkanen, V. J. Kolhinen, J. Qiu and C. A. Salgado, arXiv:hep-ph/0211239.

- [23] X. N. Wang and M. Gyulassy, Phys. Rev. Lett. **68** (1992) 1480.
- [24] M. Gyulassy and X. n. Wang, Nucl. Phys. B **420** (1994) 583 [arXiv:nucl-th/9306003].
- [25] I. Vitev and M. Gyulassy, Phys. Rev. C **65** (2002) 041902 [arXiv:nucl-th/0104066].
- [26] I. Vitev and M. Gyulassy, arXiv:hep-ph/0208108.
- [27] D. Teaney, J. Lauret and E. V. Shuryak, arXiv:nucl-th/0110037.
- [28] X. f. Zhang, G. Fai and P. Levai, arXiv:hep-ph/0205008.
- [29] R. C. Hwa and C. B. Yang, arXiv:nucl-th/0211010.
- [30] R. J. Glauber and G. Matthiae, Nucl. Phys. B **21** (1970) 135.
- [31] K. J. Eskola, V. J. Kolhinen and C. A. Salgado, Eur. Phys. J. C **9** (1999) 61 [arXiv:hep-ph/9807297].
- [32] A. Accardi and D. Treleani, Phys. Rev. D **64** (2001) 116004 [arXiv:hep-ph/0106306].
- [33] J. w. Qiu and G. Sterman, arXiv:hep-ph/0111002.
- [34] M. Gyulassy, P. Levai and I. Vitev, Phys. Rev. D **66** (2002) 014005 [arXiv:nucl-th/0201078].
- [35] For a summary of recent results on the Cronin effect see A. Accardi, *these proceedings*.
- [36] M. Gyulassy, P. Levai and I. Vitev, Nucl. Phys. B **594** (2001) 371 [arXiv:nucl-th/0006010].
- [37] M. Gyulassy, P. Levai and I. Vitev, Phys. Rev. Lett. **85** (2000) 5535 [arXiv:nucl-th/0005032].
- [38] For a summary of recent results on non-Abelian energy loss see R. Baier, P. Levai, I. Vitev, U. A. Wiedemann, *these proceedings*.
- [39] R. Baier, Y. L. Dokshitzer, A. H. Mueller and D. Schiff, JHEP **0109** (2001) 033 [arXiv:hep-ph/0106347].
- [40] M. Gyulassy, P. Levai and I. Vitev, Phys. Lett. B **538** (2002) 282 [arXiv:nucl-th/0112071].
- [41] E. Wang and X. N. Wang, Phys. Rev. Lett. **89** (2002) 162301 [arXiv:hep-ph/0202105].
- [42] C. A. Salgado and U. A. Wiedemann, Phys. Rev. Lett. **89** (2002) 092303 [arXiv:hep-ph/0204221].
- [43] S. Mioduszewski [PHENIX Collaboration], arXiv:nucl-ex/0210021.
- [44] P. Jacobs, arXiv:hep-ex/0211031.
- [45] G. J. Kunde, arXiv:nucl-ex/0211018.
- [46] F. Cooper, E. Mottola and G. C. Nayak, arXiv:hep-ph/0210391.